Hindawi
Geofluids
Volume 2019, Article ID 5489051, 12 pages
https://doi.org/10.1155/2019/5489051

Research Article

Characteristics of Bituminous Coal Permeability Response to the Pore Pressure and Effective Shear Stress in the Huaibei Coalfield in China

Lei Zhang[1], **Zhiwei Ye**[2], **Mengqian Huang**[1] **and Cun Zhang**[3]

[1]*Key Laboratory of Deep Coal Resource Mining (Ministry of Education of China), School of Mines, State Key Laboratory of Coal Resources and Safe Mining, China University of Mining & Technology, Xuzhou, Jiangsu 221116, China*
[2]*State Key Laboratory for Geomechanics & Deep Underground Engineering, China University of Mining & Technology, Xuzhou, Jiangsu 221116, China*
[3]*School of Resource and Safety Engineering, State Key Laboratory of Coal Resources and Safe Mining, China University of Mining and Technology (Beijing), Beijing 100083, China*

Correspondence should be addressed to Lei Zhang; leizhangcumt@163.com and Zhiwei Ye; cereal_god@126.com

Received 20 November 2018; Revised 6 January 2019; Accepted 12 January 2019; Published 31 March 2019

Academic Editor: Zhenjiang You

The coal permeability is known to be influenced by the pore pressure and effective stress in coal mines. In this study, the characteristics of the bituminous coal permeability response to the pore pressure and effective shear stress in the Xutuan coal mine in Huaibei Coalfield in China were investigated under different stress conditions. For this purpose, gas seepage tests with various stress levels were conducted via the original gas flow and displacement testing apparatus using bituminous coal samples from the Xutuan coal mine. The pore pressure effect on the permeability under different stress conditions was assessed by varying the pore pressure in coal samples and simulating different in situ stresses. The axial and radial pressures were controlled to study the response of coal permeability to the effective shear stress. The experimental results revealed that with an increase in pore pressure, the permeability of coal in different stress environments firstly drops and then rises. The permeability increased gradually with the effective shear stress, which trend became more pronounced when the effective shear stress exceeded zero. In case of the axial pressure exceeding the radial one, the cross shear slip was observed, for which the permeability of coal samples increased with the effective shear stress. In the opposite case, the separated shear slip was observed, with the reverse trend.

1. Introduction

China has a total of 102.3 billion m^3 of proven coalbed methane geological reserves and 47 billion m^3 of recoverable reserves, which ranks its development potential as third in the world [1]. However, the permeability of coal seam gas in China is generally low. Insofar as higher permeability implies more continuous and efficient gas release from coal seams, this parameter optimization is of great significance for the efficient mining of coalbed gas, mine gas leakage prevention and control, gas injection displacement, and other fields. In cases of roadway excavation, working face advance, or borehole drainage, the gas injection displacement influences the permeability of gas in the coal and rock masses. For low-permeability coal seam with soft coal, the gas pressure in the coal seam is rapidly reduced. The increase in the effective stress in the coal matrix reduces the opening of cracks in the coal, diminishing its permeability, causes a substantial attenuation, and so on. Therefore, the pore gas pressure and effective stress are significant factors controlling the permeability. It is necessary to carry out more in-depth experimental research to analyze the effect of these two factors on the coal permeability.

The relationship between the coal permeability and the effective stress has been substantiated by the model proposed by Palmer and Mansoori [2], which linked the effective stress with the coal matrix shrinkage and, thus, explained the effective stress reduction effect on the permeability variation from

the porosity standpoint. This negative exponential trend was confirmed by numerous researchers worldwide [3–9]. However, Connell [10] revealed that the relationship between permeability and effective force does not fully explain the relationship between the permeability, stress, and gas pressure. Zhang's [11] research in his doctoral dissertation found that under different experimental conditions, even if the effective stress is the same, the permeability of coal is quite different, and was analyzed from the angle of deviatoric stress. Besides, the axial and radial seepage experiments were carried out by Zhang et al. [12, 13], which revealed that the radial permeability was sensitive to the axial pressure variation, while the axial permeability was sensitive to the radial confining pressure variation. Most scholars only consider the effect of effective normal stress when studying the relationship between effective stress and permeability, but do not consider the effective shear stress. Therefore, the influence of effective shear stress on permeability can be analyzed from the perspective of deviatoric stress.

Jiang et al. [14] studied the relationship between the pore pressure and the permeability. Based on the semianalytical solution of the distribution law of pore gas pressure in the radial flow field, Sun [15] derived the analytical relation between the permeability coefficient of the coal seam and the gas seepage and pore pressure physical parameters. Kumar et al. [16] revealed that the He permeability increases with gas pressure under constant confining stress for both nonpropped and propped cases. Ye et al. [17] analyzed the variation pattern of permeability versus gas pressure through seepage experiments and quite accurately described it with a quadratic polynomial function. Zhao et al. [18] studied the adsorption effect on gas seepage behavior under the complex 3D stress state conditions. The results obtained strongly indicated that the permeability of coal samples increased with temperature, while a negative exponential dependence linked the permeability and effective stress dependence. Moreover, under constant confining pressure, the increment of permeability caused by the slippage effect was found to decrease exponentially with the fluid pressure [19]. Long et al. [20] experimentally studied the effect of adsorption and adsorption capacity on the coal permeability and derived the cubic polynomial fitting curve, which exactly matched the experimental results. Yin et al. [21] used the coal briquette produced by gas outburst coal to carry out seepage tests and obtained the power distribution curve of the experimental data. Cai and Yu [22] and Cai and Sun [23] conducted a theoretical study on the imbibition (which is a typical type of capillary flow) in porous media and proposed a fractal model for the elucidation of fracture mechanism and porosity. Zhang et al. [24–26] experimentally studied the effect of gas injection displacement on the coal permeability and reported that the latter could be improved after adsorbing N_2. Many scholars worldwide paid much attention to the effect of effective stress or pore pressure on the permeability. However, only a few of them attempted to perform a comprehensive analysis of permeability response to pore pressure under complex stress conditions (different effective stress, confining pressure). Furthermore, most scholars focused on the effect of effective normal stress on coal permeability, while studies on the influence of coal skeleton shear stress on the permeability are quite scarce. The effect of pore pressure on permeability is generally attributed to (i) the Klinkenberg (gas slippage) effect and (ii) the pore pressure compression effect.

In 1941, Klinkenberg [27] revealed that, in contrast to liquids, gases do not adhere to the pore walls, and their slippage along the latter gives rise to an apparent dependence of permeability on pressure. The pore pressure compression effect implies that the gas pressure in the coal fissures acts on the coal matrix and causes the coal matrix to shrink, thus increasing the seepage channel of the coal fracture and then increasing the permeability. However, the shrinkage deformation of the coal matrix is related not only to the pore pressure but also to the coal confining pressure. The extension and dilation of the fracture are limited by the increasing confining stress in the plastic zone, and the fracture system cannot enhance the permeability greatly [28]. The deformation of the coal matrix is generally evaluated by the effective stress, which combines pore pressure and confining pressure to characterize the skeleton stress of coal. The deformation of the coal matrix is accompanied by the restructuring process in the coal pore system, which affects the permeability of coal. Therefore, it is necessary to carry out permeability experiments under complex stress conditions with variable pore pressure and synthesize the effect of effective shear stress, so as to deeply study the influence of the two on coal permeability.

Given this, the characteristics of coal permeability response to the pore pressure and effective shear stress under different stress conditions observed in the Xutuan coal mine in Huaibei Coalfield in China were experimentally investigated in this paper. The experiment of gas seepage for various stress conditions was carried out with the gas flow and displacement testing apparatus developed by the authors of this study. The influence of pore pressure on permeability under different stress conditions was analyzed by varying the pore pressure in coal samples and generating different in situ stresses. The axial and radial pressures were controlled to study the characteristics of the coal permeability response to the effective shear stress. It is expected to systematically analyze the influence mechanism of the two factors on the permeability of bituminous coal and to perfect the theoretical basis for coalbed methane (CBM) production and gas injection displacement.

2. Experiment

2.1. Research Background. The Xutuan Coal Mine is located in the Mengcheng County, southwest of Suzhou City, Anhui province of China. The Xutuan coal field belongs to the Permian coal system. The relative gas emission of the mine is 22 m^3/t, and the mine belongs to the high gas mine. The coal of Xutuan coal mine is bituminous coal. 32 and 82 coal seams are the main mining seams in the mine field, and the mining area accounts for 99% of the total area.

The results of industrial analysis of coal samples from different areas of the same coal seam are often different, because of the influence of coal seam occurrence and sampling methods. It is generally believed that samples with less ash

Table 1: Maceral statistics of sampling coal seam [29].

Coal samples	Organic component (%)				R_{max} (%)
	Vitrinite	Semivitrinite	Inertinite	Exinite	
SA3	66.93	9.68	14.53	8.86	0.82
SA8	72.96	9.79	12.06	5.19	0.95

Table 2: The proximate analyses of sampling coal seam [29].

Coal samples	Mad (%)	Aad (%)	S.d (%)	P.d (%)	Vdaf (%)
SA3	1.51	18.85	0.68	0.0089	35.39
SA8	1.41	17.88	0.53	0.0112	31.93

Note: Mad: moisture content; Aad: ash content; S.d: sulfur content; P.d: phosphorus content; Vdaf: volatile matter, ad: air dried condition, daf: dry ash free condition.

can better reflect the actual situation of coal seam. Therefore, SA3 and SA8 coal samples are selected as experimental coal samples. The coal sample SA3 was derived from 32 coal seam, and the coal sample SA8 was derived from 82 coal seam. The coal petrology parameters of the main coal seams are listed in the following two tables (Tables 1 and 2).

The selected lumps of coal from the Xutuan coal mine site were placed in sealed plastic packing and brought to the laboratory. Then the coal was processed into a diameter of 50 mm and height of 100 mm experimental coal samples.

2.2. Test Equipment. The gas flow and displacement testing apparatus consists of the following subsystems: the loading system, the temperature control system, and the strain test system. The coal sample was placed in a colloid sleeve, and the confining pressure was loaded using water. The airflow displacement measuring device is composed of loading system, temperature control system, and strain measuring system. Coal samples are placed in a colloidal sleeve, and the confining pressure is loaded with water. The rubber sleeve is deformed by confining pressure to form a sealed space, which can prevent gas escaping during the experiment. Axial pressure was loaded by a fully automatic axial compression pump. The temperature of the experimental system is maintained constant by a recirculating water bath system. When the water in the high-pressure kettle is heated, the coal sample will also be heated. When the gas flows out of the coal sample, it is measured by the flowmeter and the permeability of the coal under this condition is calculated. It should be noted that the gas pressure will always be lower than the confining pressure to prevent the destruction of the sealing space of the rubber sleeve, thus generating data anomalies. Figures 1 and 2 are the schematic diagram and the physical map of the gas flow and displacement testing apparatus.

2.3. Calculation and Test Schemes

2.3.1. Calculation of Permeability. Insofar as coal is a porous medium, the gas flow in the coal seam can be roughly described by a linear seepage law. The formula of axial permeability of compressible gas can be obtained by normalizing the flow rate and pressure of Darcy's theorem permeability formula [17]:

$$K = \frac{2P_0Q_0\mu L}{A\left(P_1^2 - P_2^2\right)}, \quad (1)$$

where K is the coal permeability, mD; Q is the gas flow rate, cm^3/s; μ is the gas viscosity coefficient, Pa·s; L is the coal sample length, cm; A is the base area of the coal sample, cm^2; P_1 and P_2 are the relative gas pressures at the inlet and outlet of the raw coal sample, respectively, MPa.

2.3.2. Calculation of the Effective Shear Stress. The following formula is widely used to characterize the average effective stress in the relationship between the effective stress and the permeability in cylindrical coal samples [7, 30]:

$$\sigma' = \frac{1}{3}(\sigma_a + 2\sigma_r) - \frac{1}{2}(P_1 + P_2), \quad (2)$$

where σ' is the average effective stress, MPa; σ_a is the axial pressure, MPa; σ_r is the radial pressure, MPa; P_1 and P_2 are the inlet and outlet pressures in the coal sample, respectively, MPa.

Under the constant stress conditions, the permeability is influenced by the axial and radial pressure variations. In practice, only the effective normal stress effect is considered by the above equation, while the impact of shear stress is not taken into account. Although the stress in the coal sample is hard to assess, the maximum and minimum principal stresses in the axial and radial planes are considered as the axial and radial pressures, respectively. Thus, the average effective shear stress of coal samples is assessed.

$$\tau' = \frac{\sigma_a - \sigma_r}{2}, \quad (3)$$

where τ' is the average shear stress, MPa.

The effect of the average effective shear stress of the coal sample on the permeability is accounted for by controlling the test conditions. The shear stress can be varied to carry out the permeability test under constant normal stress, and then the coal permeability variation with the average effective shear stress can be obtained. Next, the permeability test results obtained at the same effective shear stress values are compared.

2.3.3. Test Schemes. The pore pressure effect on the permeability under various pressure conditions was studied on coal samples SA3 and SA8 in CH_4 environments, respectively. The seepage tests under the following three stress conditions were conducted as well: (1) tests with a constant confining pressure and varying inlet pore pressure ($\sigma_r = \sigma_a = \text{constant}$); (2) tests with a constant average effective stress and varying inlet pore pressure ($\sigma' = \sigma_a - (P_1 + P_2)/2 = \text{constant} \cap \sigma_r = \sigma_a$); (3) tests with a constant inlet effective stress and varying inlet pore pressure ($(\sigma' = \sigma_a - P_1) = \text{constant} \cap \sigma_r = \sigma_a$).

The respective characteristics of permeability response to the internal forces of the coal skeleton were experimentally obtained using the test schemes plotted in Figures 3–5, where the evolutions of axial, radial, and inlet pore pressures are indicated by circles, crosses, and triangles, respectively. The

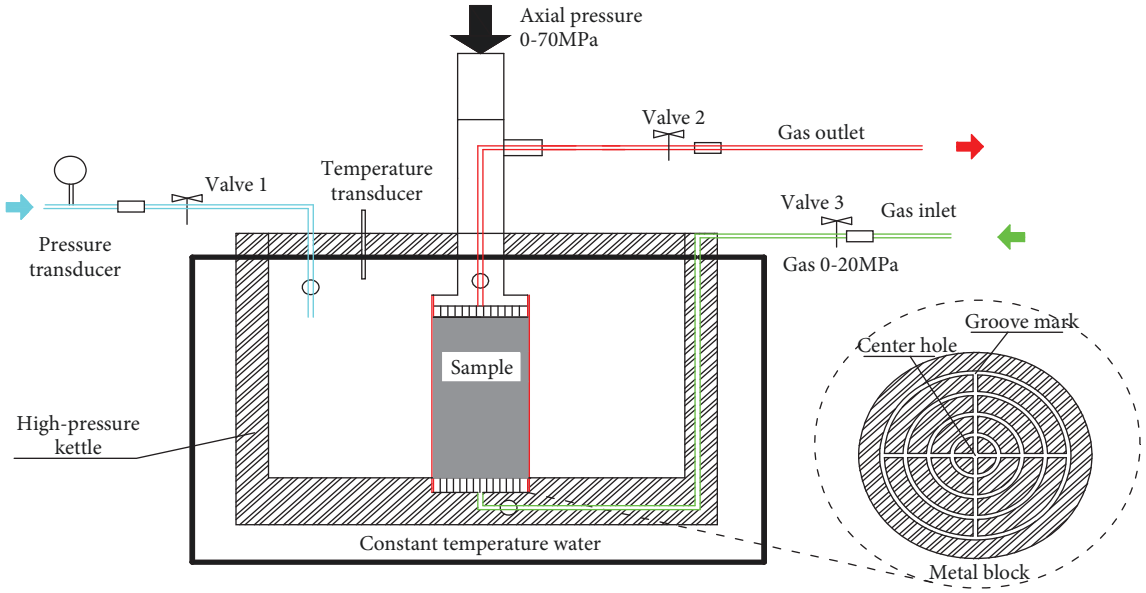

Figure 1: Schematic diagram of the gas flow and displacement testing apparatus.

Figure 2: The gas flow and displacement testing apparatus.

permeability tests with control of the effective normal and shear stresses in coal samples were also carried out, according to the test schemes depicted in Figures 6 and 7, respectively.

3. Experimental Results and Discussion

3.1. Experimental Results and Analysis of Pore Pressure on Coal Samples. The experimental dependences of the coal sample permeability versus inlet pressure under constant confining pressure values were obtained and plotted in Figure 8, where positive and negative confining pressure values correspond to the loading and unloading stages of the coal samples, respectively.

The preliminary analysis of Figure 8 reveals that (i) all permeability curves exhibit a decreasing trend at the initial stage, which is followed by a rising one, and (ii) all permeability curve corresponding to the sample unloading stage are lower than those of the loading one at the confining pressure values. These two findings can be substantiated as follows.

A constant confining pressure is equivalent to imposing constant confining stresses to the coal sample, that is, gradually increasing the inlet pressure under the condition that the total stress remains unchanged. In the case of the constant stress, an increase in the pore fluid pressure is expected to reduce stresses in the coal body skeleton, leading to the fracture expansion by the fluid extrusion, thus increasing the permeability. However, the experimental results on pore pressure seepage under constant confining pressure show a different pattern: the permeability decreases first and then increases with the pressure. By comparing the permeability curves constructed under different confining pressures, it can be seen that larger confining pressures result in more pronounced declining trend at the early stage. Such decline can be attributed to the Klinkenberg effect (KE) of pore gas flow and to the fact that too low pore pressures have a weak impact on the coal skeleton deformation. Gas flow in porous media is quite different from liquid flow due to the large gas compressibility and pressure-dependent effective permeability [31]. This explains why higher confining pressures promote the initial decreasing trend of permeability curves.

The KE of gas flow in a porous medium refers to the fact that the velocity of gas molecules on the pore surface is almost the same as that in its center. This is due to the small molecular binding force between the gas and the solid. On the other hand, the gas molecules in the adjacent layers have kinetic energy exchange, which leads to the homogenization of the molecular layer of the gas in the channel wall and the molecular layer of the center of the channel. The influencing factors of KE (gas slippage effect) are assessed via the following equation [27]:

$$K_{\infty} = \frac{K_g}{1 + (b/\bar{p})}, \tag{4}$$

where K_g is the permeability of a porous medium with an average pore pressure of $\bar{p}$, mD; K_{∞} is the Klinkenberg permeability, also known as the equivalent liquid permeability, which is independent of the pore pressure, mD, while b is a coefficient related to the pore structure of rock and the mean free path of gaseous molecules, which is also referred to as the Klinkenberg coefficient. The relationship between average

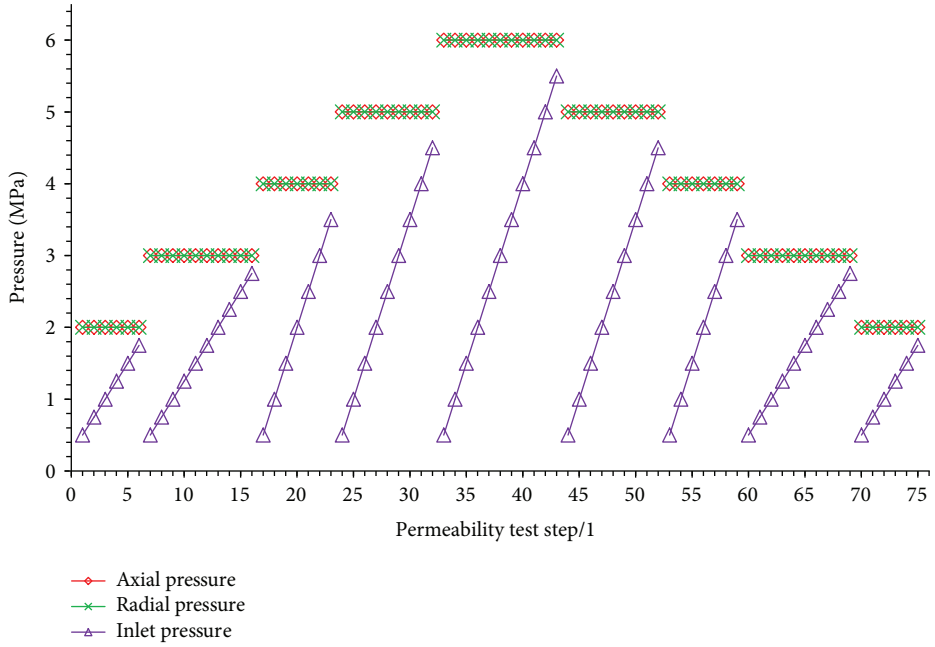

Figure 3: Tests on the pore pressure effect on the permeability under constant confining pressure.

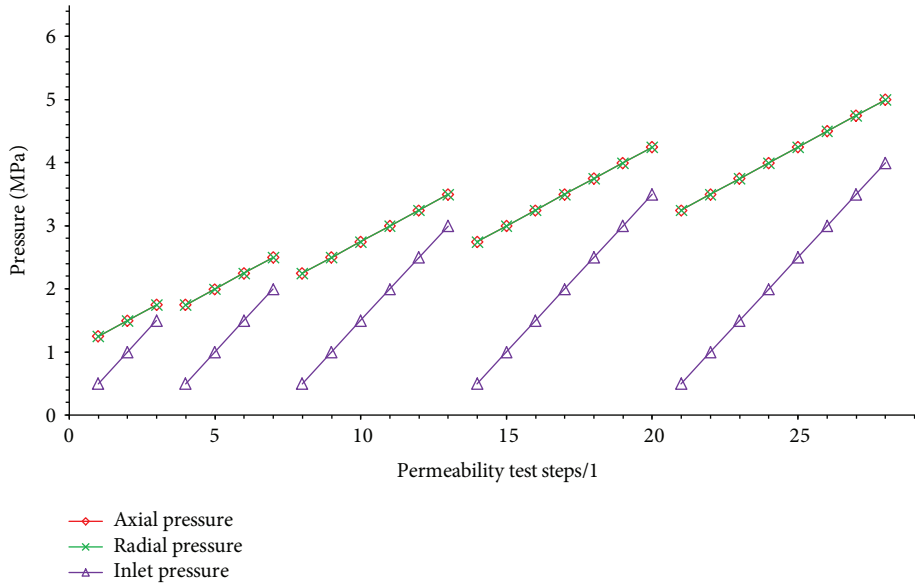

Figure 4: Tests on the pore pressure effect on the permeability under constant average effective stress.

effective stress and permeability can be obtained by substituting parameters related to b. It can be derived as follows [17]:

$$K_g = \left(1 + \frac{4ck_BT}{\sqrt{2}\pi r d^2 \bar{p}}\right) K_\infty, \tag{5}$$

where c is a proportional coefficient; T is thermodynamic temperature, K; k_B is the Boltzmann constant; d is the diameter of percolation gas molecule, m.

It can be seen from equation (5) that the KE influencing factors, in the decreasing order of their significance, are the average pore pressure, the pore radius of the porous medium, and the molecular diameter of the percolation gas at constant temperature. Smaller pore pressures result in higher deviations of the gas permeability from the equivalent liquid permeability, as well as in a more pronounced gas slippage effect. Therefore, the decreasing trend at the initial stage of the permeability curve in Figure 8 has the following explanation. Because the gas slippage effect is the most pronounced at low gas pressures, the gas permeability sharply increases with the equivalent liquid permeability. With an increase in the gas pressure, the slippage effect gradually weakens, and the gas permeability increase

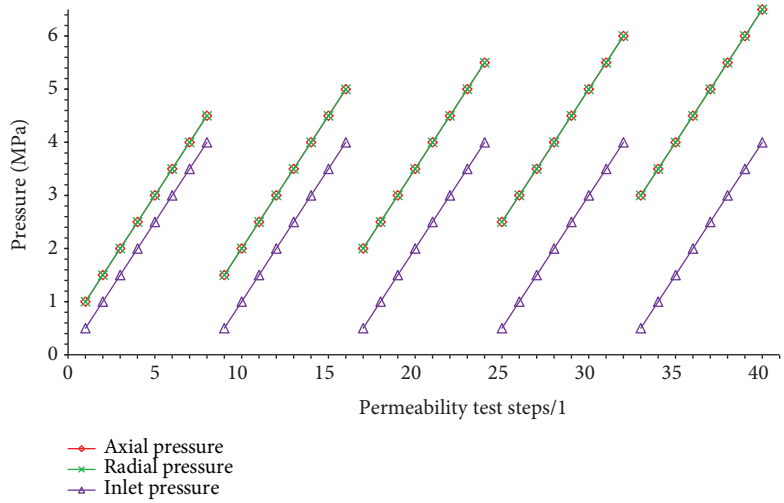

Figure 5: Tests on the pore pressure effect on the permeability under constant inlet effective stress.

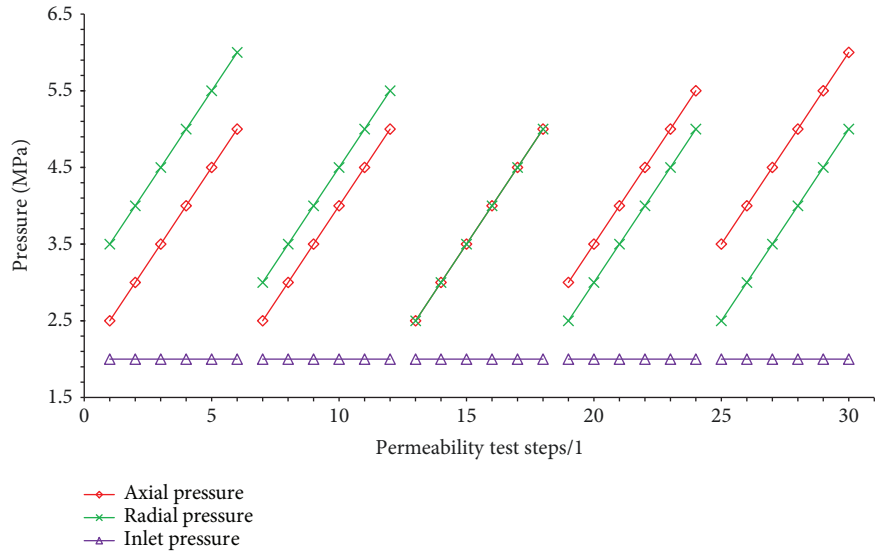

Figure 6: Tests on the pore pressure effect on the permeability under constant effective shear stress.

is slowly saturated, as compared to that of the equivalent liquid. Besides, an increase in the confining pressure will reduce the pore radii of coal samples and further enhance the slippage effect in coal. Thus, the larger the confining pressure, the more pronounced the decreasing trend of the initial portions of permeability curves.

Based on the above analysis, permeability curves at constant confining pressure can be subdivided into three portions and respective stages.

(1) The KE stage, which is the initial stage of low pore pressures, at which the seepage characteristics of coal are mainly affected by the KE, and the permeability of coal decreases with pore pressure

(2) Stable seepage stage, wherein the coal permeability is slightly affected by the pore pressure growth. At this stage, the KE is gradually saturated to almost zero effect on permeability, and the pore pressure increases slowly, but the impact of the coal and crack opening is very weak. Therefore, this is a stable stage with a slight permeability variation

(3) Percolation penetration stage, at which any increase in pore pressure will have a significant impact on the structural damage and coal skeleton deformation. At this stage, the inlet pressure of the coal sample gradually approaches to the simulated ground stress, the pore pressure makes the coal skeleton compressed and deformed, and the opening of pore channel cracks increases. The coalescence of some nonconnected pores may occur with gas pressure rise, resulting in the gas penetration. The permeability increases rapidly with the growth of pore pressure

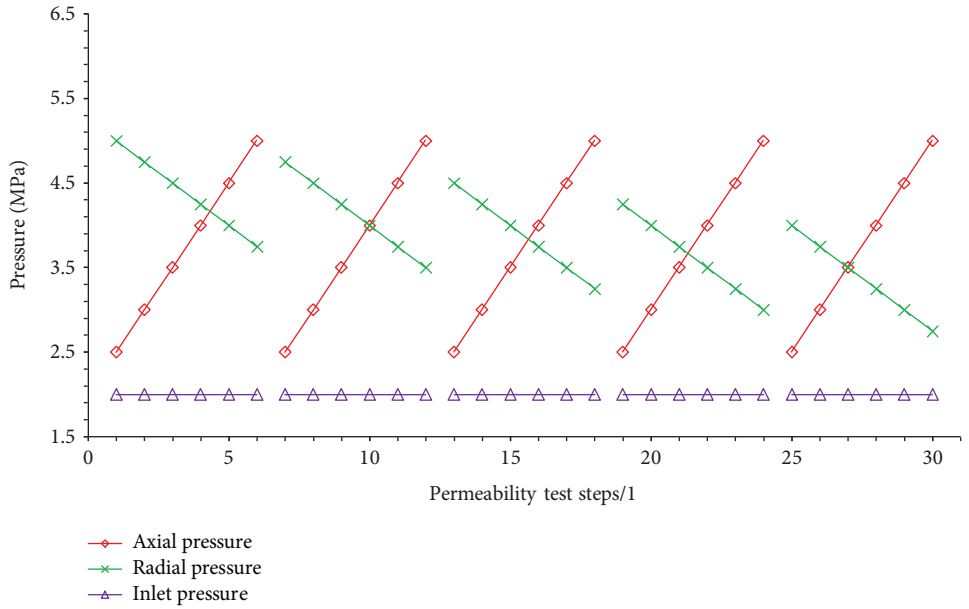

Figure 7: Tests on the pore pressure effect on the permeability under constant average effective normal stress.

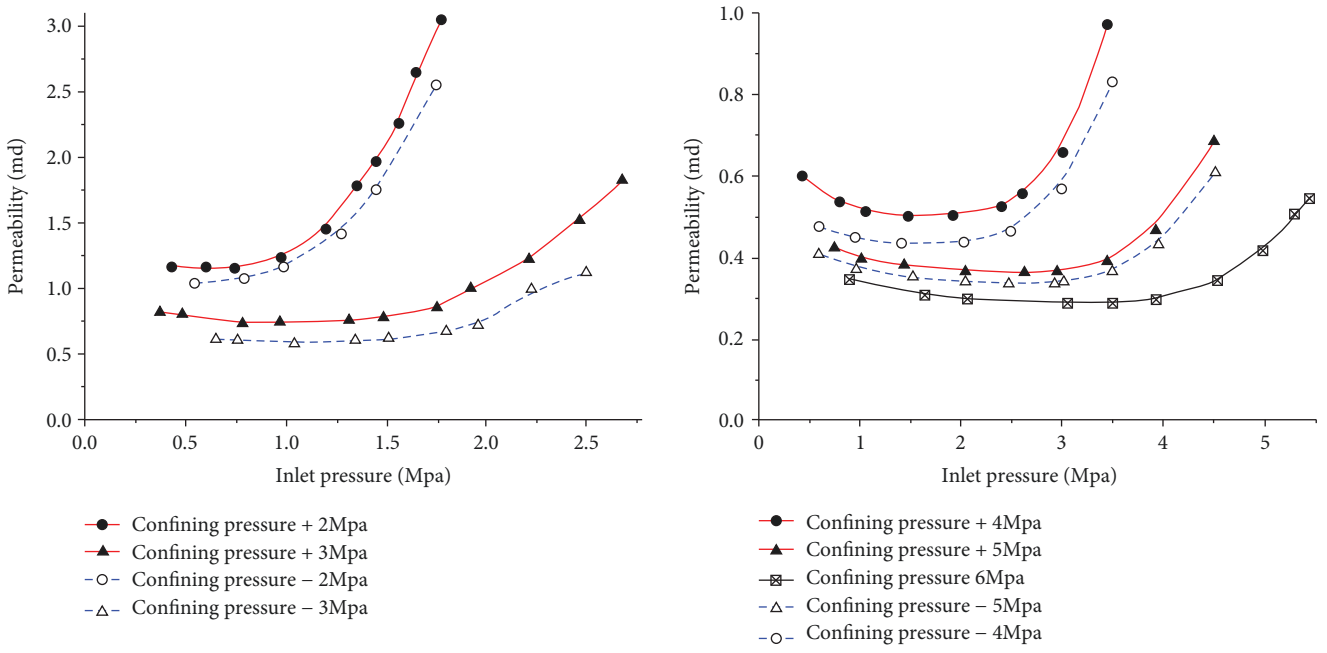

Figure 8: Test results on the pore pressure seepage under constant confining pressure.

The other finding made from Figure 8 was that the permeability curves at the unloading path are always lower than those at the loading path. Because coal is a typical plastic material, according to the principle of elastic-plastic mechanics, the stress-strain relationships of plastic materials depend on time and may feature multiple values. Under the same stress, the strain values may vary due to different loading and unloading processes. Therefore, the deformation of the solid skeleton and the expansion and contraction of the microporous fracture depend not only on the stress level and the material properties but also on the loading and unloading histories. The porosity characteristics of coal samples directly influence the gas permeability. The permeability curves corresponding to the unloading and loading paths may feature some high-pressure loads, which lead to the compression and closure of some microporous channels. After unloading, the opening of these microporous channels will exhibit a hysteresis loop phenomenon, and the longer the loading history, the more pronounced the hysteresis loop.

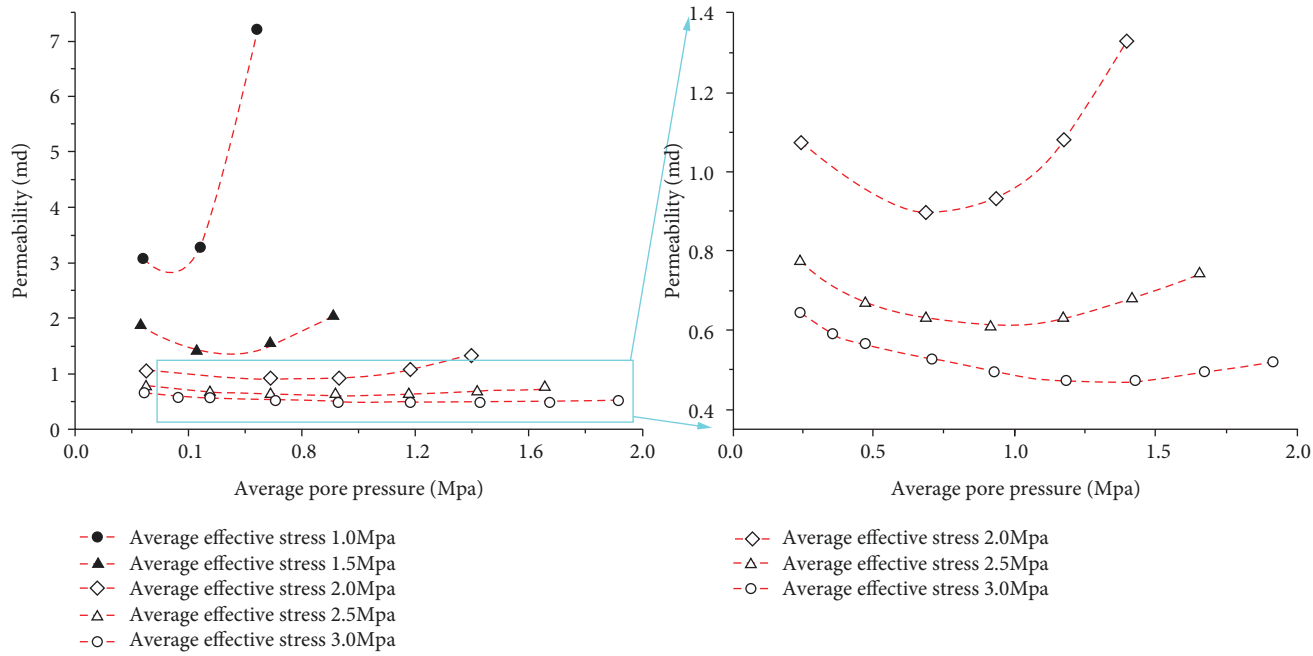

Figure 9: Test results on the pore pressure seepage under constant average effective stresses.

In fact, when the confining pressure is constant, the curve of permeability changing with the entrance pore pressure is the result of the interaction of pore pressure and effective stress. When the entrance pore pressure increases, the average pore pressure increases, the average effective stress decreases, and the permeability increases under the combined action of the two. In order to study the effect of pore pressure on coal permeability, it is necessary to exclude the effect of effective stress changes. If the effective stress of the coal sample is constant and falls into the elastic range of the coal sample skeleton deformation, the latter will be stable, and the fracture pattern will not change. Moreover, if the KE and the capillary condensation of coal are excluded, the permeability will not vary. The respective tests under constant mean and inlet effective stress conditions were performed to verify the above theoretical concept.

It was quite problematic to maintain constant values of the effective stress of coal samples under varying pore pressure conditions. The gas seepage tests with constant average effective stress values were carried out by keeping constant the difference between the radial and average pore pressures and varying the inlet pressure continuously. The constant inlet effective stress values were achieved by holding constant the difference between the radial and inlet pressures and varying the inlet pressure consistently in the respective gas seepage tests. The curves of permeability of coal samples under constant average and inlet effective stresses are plotted in Figures 9 and 10, respectively.

Although the average effective stresses of coal samples are constant, the difference between the inlet and outlet effective stress values increases. As shown in Figure 9, permeability curves firstly show a decreasing trend, which is followed by an increasing one, regardless of the average effective stress values. In fact, this decreasing trend implies that the lower is the pore pressure caused by the gas slippage effect, the higher is the gas permeability. The increasing trend in the later period of the permeability curve is presumed to be related to the heterogeneity of the microdeformation caused by the increased difference between the inlet and outlet effective stress values in coal samples. Thus, with the growth of pore pressure, although the average effective stress remains unchanged, the difference between the effective stresses at the inlet and the outlet of the coal sample increases continuously. The corresponding strain/deformation increase in the coal sample inlet and outlet leads to the rise of permeability.

When the effective inlet stress of samples is constant, the stress of the coal sample skeleton increases gradually with the pore pressure. As shown in Figure 10, the permeability decreases with the growth of inlet pressure. In fact, the decreasing trend of permeability is caused by two factors. On the one hand, the lower the pore pressure is, the higher is the measured gas permeability over that induced by the gas slippage effect. On the other hand, the inlet fluid pressure keeps increasing, and the effective stress of coal sample keeps growing under the condition that the effective inlet stress remains unchanged. The compression of coal skeleton leads to the contraction of cracks, which leads to the permeability reduction.

Besides, the common features of the permeability curves in Figures 8–10 are that, with an increase in the confining pressure or effective stress, the variation of permeability with the pore pressure and inlet pressure is becoming smaller and smaller. In other words, the growth of confining pressure or effective stress gradually weakens the sensitivity of permeability to the pore pressure and inlet pressure.

3.2. Analysis of Seepage Test Results with Different Effective Stress Values. Insofar as no noticeable difference in the permeability of the SA3 and SA8 coal samples was observed, the permeability test results are listed and analyzed only for

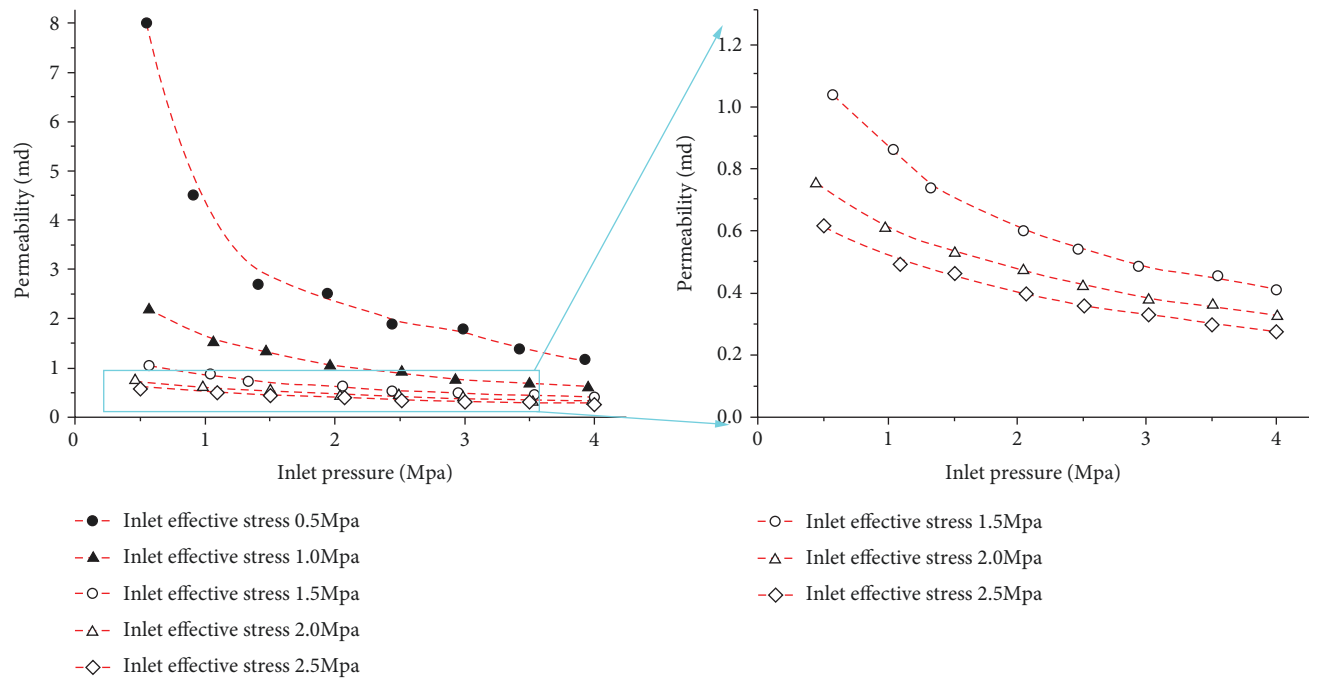

Figure 10: Test results on the pore pressure seepage under constant inlet effective stresses.

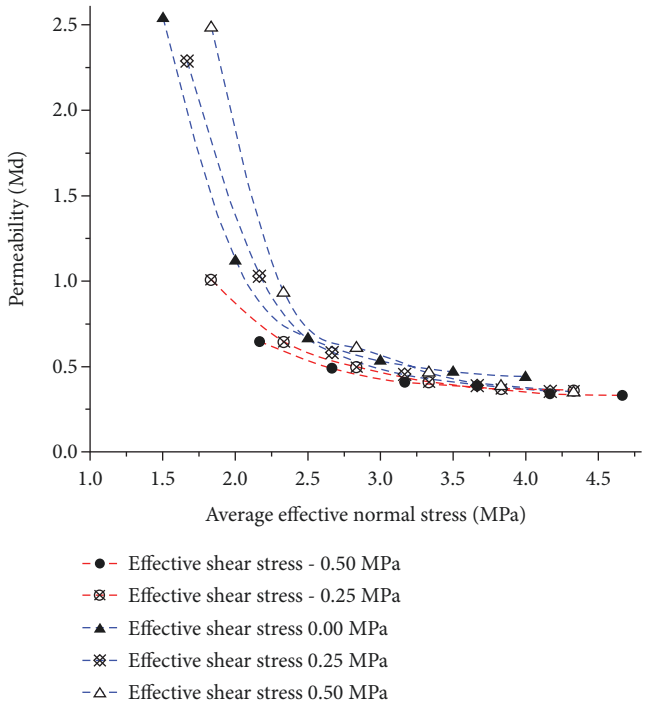

Figure 11: The seepage test results obtained under constant effective shear stress conditions.

SA3. The test results obtained under constant effective shear and normal stress conditions are depicted in Figures 11 and 12, respectively.

According to Figure 11, under constant effective shear stress conditions, the permeability of coal sample decreases with the average effective normal stress. The initially strong declining trend of the permeability curve becomes saturated with an increase in the average effective normal stress. Noteworthy is that when the average effective normal stress is in the range of 1.5-2.5 MPa, the permeability curve with larger effective shear stress is always higher than that with a smaller one. When the average effective normal stress exceeds 2.5 MPa, there is no noticeable difference in permeability curves constructed under different effective shear stress values. The effective normal stress represents the internal compressive force of the coal skeleton. This compressive effect will inevitably lead to the compression of fractured coal masses and reduce their permeability. When the average effective normal stress increases in the initial stage, the cracks in the coal body change from opening to closing, and the permeability change is more sensitive. However, as the stress continues to increase, the cracks in the coal body remain closed, and there is no sign of expansion, so the permeability curve changes gently. Fitting formulas for different curves are shown in Table 3. The relationship between permeability and effective positive stress is negative exponential function, which is the same as that of other scholars. Compared with different effective shear stress permeability curves, the permeability increases gradually with the increase of effective shear stress, but there are fewer data points in the figure, so further analysis is made in subsequent experiments.

In this study, additional seepage tests of the permeability response to the effective shear stress were carried out with constant average effective normal stress values. The experimental results are shown in Figure 12: the permeability curve exhibits a gradual rise with the effective shear stress when the effective shear stress is negative (i.e., the axial pressure is less than the radial one), but this increasing trend of permeability is not strongly pronounced. When the effective shear stress attains positive values (the axial pressure exceeds the radial one), this increase becomes more evident.

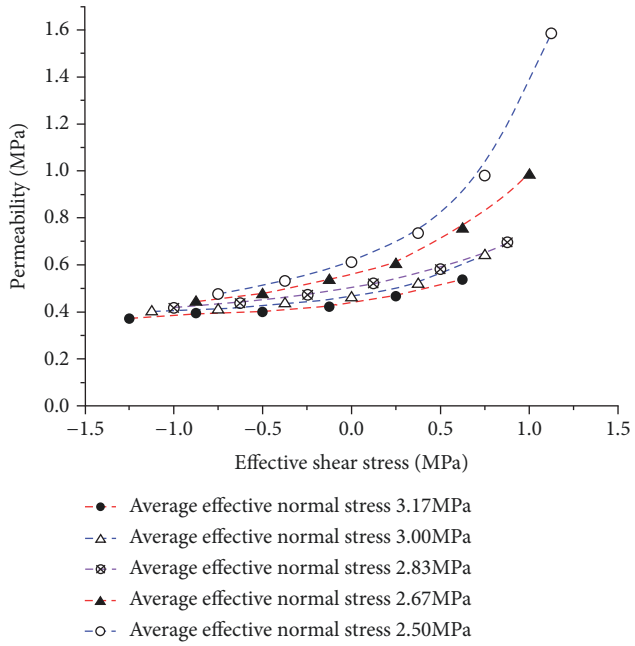

Figure 12: The seepage test results obtained under constant effective normal stress conditions.

Table 3: Fitting formula.

The effective shear stress (MPa)	Fitting formula	R^2
-0.5	$K = 5.05e^{(-1.27\sigma')} + 0.32$	0.99
-0.25	$K = 11.03e^{(-1.53\sigma')} + 0.34$	0.99
0	$K = 61.28e^{(-2.25\sigma')} + 0.45$	0.99
0.25	$K = 65.14e^{(-2.11\sigma')} + 0.36$	0.99
0.5	$K = 228.25e^{(-2.56\sigma')} + 0.39$	0.99

From the point of view of coal skeleton stress, the effective normal stress of coal is constant, which shows that the compressive stress of coal skeleton has not changed. But at this time, the increase of effective shear stress leads to the increase of permeability, which indicates the deformation of coal skeleton and internal cracks. Even, local fracture of coal body skeleton may occur, and internal cracks develop further due to the influence of shear slip. Concerning the stress sensitivity, consider the case where the effective shear stress is negative, i.e., the radial pressure is higher than the axial one. If the average effective normal stress is kept constant, the coal skeleton has the same compression state, whereas the effective shear stress represents the intensity of shear slip in the coal skeleton. So, in this case, the shear slip degree caused by the effective shear stress is quite intense, and the coal sample permeability is high. Under the same effective normal stress conditions, if the axial pressure is less than the radial one, the shear slip degree caused by the effective shear stress is less intense, and the coal permeability is somewhat lower, but this trend is not apparent. Besides, under negative effective shear conditions, the permeability curves change slightly, while under a positive one, this change is more drastic. Therefore, the permeability is more sensitive to the axial pressure, which acts parallel to the flow direction, and shows low sensitivity to the vertical radial pressure of the seepage flow. The fitting formulas are given in Table 4. The relationship between permeability and average effective shear stress is exponential function and fits well.

Table 4: Fitting formula.

Average effective normal stress (MPa)	Fitting formula	R^2
3.17	$K = 0.07e^{(1.42\tau')} + 0.37$	0.99
3	$K = 0.06e^{(1.77\tau')} + 0.4$	0.99
2.83	$K = 0.12e^{(1.1\tau')} + 0.38$	0.99
2.67	$K = 0.15e^{(1.34\tau')} + 0.4$	0.99
2.5	$K = 0.12e^{(1.95\tau')} + 0.47$	0.99

The compression effect of the coal skeleton is the primary source of the coal sample permeability reduction with the average effective normal stress. The shear slip degree of coal skeleton characterized by effective shear stress also affects the permeability of coal samples. When the effective normal stress is constant, the compression effect of the coal skeleton will remain unchanged, but it will still be deformed by the effective shear stress, and the cracks will dislocate or even extend. The influencing factors of coal body are the magnitude and direction of effective shear stress.

When the axial pressure of coal sample is larger than the radial one, the effective shear stress is positive and the coal sample shows cross slip (Figure 13(a)). In this case, the permeability increases with the effective shear stress, which represents the intensity of shear slip in the coal skeleton. When the radial pressure of coal samples is higher than the axial pressure, the effective shear stress is positive and the separated slip will appear (Figure 13(b)). In this case, the permeability decreases with the effective shear stress, but the decreasing trend is less apparent.

4. Conclusions

(1) Under constant confining pressure (which models the ground stress), the permeability of coal sample decreases first and then increases with the inlet pore pressure (which simulates the coal seam gas pressure). Permeability curves at constant confining pressure can be subdivided into three portions and respective stages, the KE stage, stable seepage stage, and percolation penetration stage. This is the result of the interaction of effective stress and pore pressure

(2) The permeability curves at the unloading path are always lower than those at the loading path

(3) When the average effective stress is constant, the permeability curve exhibits a V-shaped portion versus the pore pressure

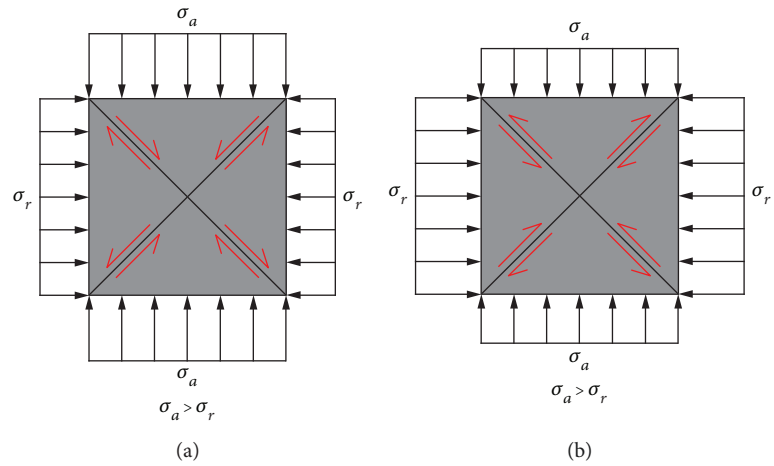

Figure 13: Various slip trends observed under different combinations of axial and radial pressures.

(4) With an increase in confining pressure and effective stress, the variation of permeability decreases with pore pressure and inlet pressure. In other words, the growth of confining pressure and effective stress leads to the gradually saturated sensitivity of permeability to the pore pressure inlet pressure

(5) The permeability gradually increased with the effective shear stress, but this increasing trend was not apparent when the effective shear stress was negative. With the attainment of positive values by the effective shear stress, the above trend gradually became more pronounced. The relationship between permeability and average effective shear stress is exponential function and fits well

(6) The coal sample permeability increased with the effective shear stress when its axial pressure exceeds the radial one. In the opposite case, the reverse trend was observed. Finally, the coal sample permeability was found to be more sensitive to the effective shear stress under cross shear slip conditions than under the separated ones

Data Availability

The data used to support the findings of this study are available from the corresponding author upon request.

Conflicts of Interest

The authors declare that there are no conflicts of interest regarding the publication of this paper.

Acknowledgments

This research is supported by the Fundamental Research Funds for the Central Universities (2017XKZD06) and the Priority Academic Programme Development of Higher Education Institutions in Jiangsu Province.

References

[1] F. Zhou, T. Xia, X. Wang, Y. Zhang, Y. Sun, and J. Liu, "Recent developments in coal mine methane extraction and utilization in China: a review," *Journal of Natural Gas Science and Engineering*, vol. 31, pp. 437–458, 2016.

[2] I. Palmer and J. Mansoori, "How permeability depends on stress and pore pressure in coalbeds: a new model," *SPE Reservoir Evaluation and Engineering*, vol. 1, no. 6, pp. 539–544, 2013.

[3] Y. Li, D. Tang, H. Xu, Y. Meng, and J. Li, "Experimental research on coal permeability: the roles of effective stress and gas slippage," *Journal of Natural Gas Science and Engineering*, vol. 21, pp. 481–488, 2014.

[4] J. Zou, W. Chen, D. Yang, H. Yu, and J. Yuan, "The impact of effective stress and gas slippage on coal permeability under cyclic loading," *Journal of Natural Gas Science and Engineering*, vol. 31, pp. 236–248, 2016.

[5] X. Li and G. Yin, "Relationship between effective volumetric stress and permeability of gas-filled coal," *Journal of Chongqing University*, vol. 34, no. 8, pp. 103–108, 2011.

[6] G. Yin, W. Li, M. Li, X. Li, B. Deng, and Z. Jiang, "Permeability properties and effective stress of raw coal under loading-unloading conditions," *Journal of China Coal Society*, vol. 39, no. 8, pp. 1497–1503, 2014.

[7] S. Peng, J. Xu, Y. Tao, and M. Cheng, "Coefficient of sensitiveness between permeability and effective pressure of coal samples," *Journal of Chongqing University*, vol. 32, no. 3, pp. 303–307, 2009.

[8] H. Chen, Y. Cheng, T. Ren, H. Zhou, and Q. Liu, "Permeability distribution characteristics of protected coal seams during unloading of the coal body," *International Journal of Rock Mechanics and Mining Sciences*, vol. 71, pp. 105–116, 2014.

[9] L. Zhang, Y. Wu, H. Pu, X. He, and P. Li, "The migration of coalbed methane under mining pressure and air injection: a case study in China," *Geofluids*, vol. 2018, Article ID 4034296, 14 pages, 2018.

[10] L.-D. Connell, "A new interpretation of the response of coal permeability to changes in pore pressure, stress and matrix shrinkage," *International Journal of Coal Geology*, vol. 162, pp. 169–182, 2016.

[11] C. Zhang, *Coupling mechanism of stress-fracture-flow in high gas coal seam group and its impact on pressure relief extraction*,

China University of Mining and Technology, 2017, http://kns.cnki.net/kns/brief/default_result.aspx.

[12] L. Zhang, C. Zhang, S. Tu, H. Tu, and C. Wang, "A study of directional permeability and gas injection to flush coal seam gas testing apparatus and method," *Transport in Porous Media*, vol. 111, no. 3, pp. 573–589, 2016.

[13] C. Zhang, S. Tu, L. Zhang, and M. Chen, "A study on effect of seepage direction on permeability stress test," *Arabian Journal for Science and Engineering*, vol. 41, no. 11, pp. 4583–4596, 2016.

[14] J. Xu, J. Cao, B. Li, T. Zhou, M. Li, and D. Liu, "Experimental research on response law of permeability of coal to pore pressure," *Chinese Journal of Rock Mechanics and Engineering*, vol. 32, no. 2, pp. 225–230, 2013.

[15] S. Peide, "A new method for calculating the gas permeability of a coal seam," *International Journal of Rock Mechanics and Mining Sciences & Geomechanics Abstracts*, vol. 27, no. 4, pp. 325–327, 1990.

[16] H. Kumar, D. Elsworth, J.-P. Mathews, and C. Marone, "Permeability evolution in sorbing media: analogies between organic-rich shale and coal," *Geofluids*, vol. 16, no. 1, 55 pages, 2016.

[17] Z. Ye, L. Zhang, D. Hao, C. Zhang, and C. Wang, "Experimental study on the response characteristics of coal permeability to pore pressure under loading and unloading conditions," *Journal of Geophysics and Engineering*, vol. 14, no. 5, pp. 1020–1031, 2017.

[18] Y. Zhao, Y. Hu, D. Yang, and J. Wei, "The experimental study on the gas seepage law of rock related to adsorption under 3-D stresses," *Chinese Journal of Rock Mechanics and Engineering*, vol. 18, no. 6, pp. 651–653, 1999.

[19] X. Fu, D. Li, Y. Qin, B. Jiang, W. Wang, and G. Li, "Experimental research of influence of coal matrix shrinkage on permeability," *Journal of China University of Mining & Technology*, vol. 31, no. 2, pp. 129–131, 2002.

[20] Q. Long, X. Zhao, D. Sun, and Y. Zou, "Experimental study on coal permeability by adsorption," *Journal of China Coal Society*, vol. 33, no. 9, pp. 1030–1034, 2008.

[21] G. Yin, X. Li, H. Zhao, X. Li, and X. Jing, "Experimental study of effect of gas pressure on gas seepage of outburst coal," *Chinese Journal of Rock Mechanics and Engineering*, vol. 28, no. 4, pp. 697–702, 2009.

[22] J. Cai and B. Yu, "A discussion of the effect of tortuosity on the capillary imbibition in porous media," *Transport in Porous Media*, vol. 89, no. 2, pp. 251–263, 2011.

[23] J. Cai and S. Sun, "Fractal analysis of fracture increasing spontaneous imbibition in porous media with gas-saturated," *International Journal of Modern Physics C: Computational Physics and Physical Computation*, vol. 24, no. 8, article 1350056, 2013.

[24] L. Zhang, N. Aziz, T. Ren, J. Nemcik, and S. Tu, "Nitrogen injection to flush coal seam gas out of coal: an experimental study," *Archives of Mining Sciences*, vol. 60, no. 4, pp. 1013–1028, 2015.

[25] L. Zhang, T. Ren, N. Aziz, and S. Tu, "Coal sorption characteristics and coal surface tension," *International Journal of Oil Gas & Coal Technology*, vol. 8, no. 3, p. 336, 2014.

[26] L. Zhang, T. Ren, N. Aziz, and C. Zhang, "Evaluation of coal seam gas drainability for outburst-prone and high-CO2-containing coal seam," *Geofluids*, vol. 2019, Article ID 3481834, 14 pages, 2019.

[27] L.-J. Klinkenberge, "The permeability of porous media to liquids and gases," *Drilling and Production Practice*, vol. 2, no. 2, pp. 200–213, 1941.

[28] H. Zhou, J. Gao, K. Han, and Y. Cheng, "Permeability enhancements of borehole outburst cavitation in outburst-prone coal seams," *International Journal of Rock Mechanics and Mining Sciences*, vol. 111, pp. 12–20, 2018.

[29] L. Zhang, Z. Ye, M. Li, C. Zhang, Q. Bai, and C. Wang, "The binary gas sorption in the bituminous coal of the Huaibei Coalfield in China," *Adsorption Science & Technology*, vol. 36, no. 9-10, pp. 1612–1628, 2018.

[30] Q. Huang, G. Yin, Y. Jiang, and J. Yi, "Gas seepage characteristics of briquette samples in a stress field," *Journal of Chongqing University*, vol. 31, no. 12, pp. 1436–1440, 2008.

[31] W.-C. Zhu, J. Liu, J.-C. Sheng, and D. Elsworth, "Analysis of coupled gas flow and deformation process with desorption and Klinkenberg effects in coal seams," *International Journal of Rock Mechanics and Mining Sciences*, vol. 44, no. 7, pp. 971–980, 2007.